Image Analysis Based on Var-Lstm Method for Air Quality Prediction

Dr. M. Seshashayee [1], R. Udaya Bharathi [2]

1. Assistant Professor, Department of Computer Science, GITAM (Deemed to be University), Vishakhapatnam, Andhra Pradesh, India. Emailid:smaruvada@gitam.edu.

2. Research Scholar, Department of Computer Science, GITAM (Deemed to be University), Vishakhapatnam, Andhra Pradesh, India. Emailid: bharathi.es09@gmail.com.

Article Info
Page Number: 6562-6571
Publication Issue:
Vol. 71 No. 4 (2022)

Article History
Article Received: 25 March 2022
Revised: 30 April 2022
Accepted: 15 June 2022

Abstract
Data analysis and computer vision are two strong technologies that may aid us in accomplishing activities that would otherwise need more time and effort. Therefore, the first step in saving the environment should be to check air quality, particularly in developing nations. Current methods for gauging air quality need expensive, specialized instruments and infrastructure. Therefore, it might be challenging, if not impossible, to provide air quality data for far-flung locations or attractive regions, even inside cities, owing to the high price or technical complexity of the equipment required. Based on an investigation of several publicly accessible photographs of the surroundings of Beijing, Shanghai (China), and Phoenix, the authors of this paper offer a method for quantifying PM air pollution (US). The photos were processed to extract six elements that were then utilized in conjunction with other variables such as the time of day, location, and weather to forecast the $PM^{2.5}$ index. This was achieved by using deep learning techniques, namely the training of a VAR-LSTM model on the aforementioned picture dataset. The results show that PM prediction is feasible using the image analysis technique.$_{2.5}$.

I. INTRODUCTION:

The discharge of chemicals into the air that are bad for human health and the environment as a whole is what is meant by the phrase "air pollution." The manufacturing sector, particularly in emerging economies like India, China, Afghanistan, Argentina, and others, has expanded at an unprecedented rate during the last decade. Despite the fact that industrialisation has helped stabilize the economies of many nations, it has also had a negative impact on the air quality there. The list of relevant countries is topped by China, with India coming in at a close second. When we talk about "air pollution," we mean when dangerous compounds are released into the air and have an adverse effect on people and the environment. This article discusses a few of the various causes of air pollution.

1. “Most air pollution comes from energy use production.
2. Burning fossil fuels releases gases and chemicals into the air.
3. Air pollution in the form of carbon dioxide and methane raises the earth’s temperature.”

4. Moreover, the additional heat contributes to an already problematic kind of air pollution: Higher levels of UV light and higher temperatures both contribute to the formation of smog.

Particulate matter (PM) pollution often has a negative impact on visibility because it scatters sunlight. "It is easy for the typical person to tell the difference between a clear and hazy sky, but it is much more difficult to discern between hazy skies caused by particle matter (PM) and fog, and to measure the degree of PM pollution. There is now a new possibility to categorize and analyze airborne particles exclusively on digital photography, thanks to the widespread availability of high-quality digital cameras and the ever-increasing computational power for advanced image processing using even a mobile device. Wang et al. [1] in

vestigated air quality using a photometric method that estimates light extinction. However, airborne PM affects a photograph by scattering light in a complex way that varies with the position and angle of the camera, the distance between the camera and the objects, and the weather conditions; this has a variety of effects, including blurring the images of distant objects, discoloring the sky, and reducing the image contrast [2].Accurate PM evaluation needs us to take into account a number of picture attributes and the circumstances under which the images were recorded.

Based on the extraction of six picture properties—transmission, sky smoothness and color, whole image and local image contrast, and image entropy—we" present a method for identifying and measuring PM pollution.When analyzing the relationship between PM levels and other variables, we also take into account the time, location, and meteorological conditions of each shot. The PM level in images taken in Beijing, Shanghai, and Phoenix over the course of a year is predicted using a regression model trained with these characteristics. Many modern smartphones have high-resolution cameras and robust processing capacity; these features might be put to use to identify and measure PM2.5 in the air simply by analyzing photos taken in the environment.

This paper should be organized as follows. The optical model of a blurred picture was first presented. Next, the model analysis led to the extraction of many features from the hazy photos, which were then used to train and predict the PM index through support vector regression. Finally, we will assess the results and talk about how we might make the current technique more precise.

II. RELATED WORK:

There has been a lot of research into using image analysis to anticipate air pollution levels and air quality (prediction of AQI value) and to estimate suspended particles like pm2.5, SO2, NO2, etc.

Athanasiadis [3] suggested a neurocomputing classifier model for O3 levels using meteorological data, specifically a -fuzzy-lattice fuzzy-fuzzy-lattice lattice.

Kalapanidas[4] used meteorological data to suggest a classifier model that divides pollution levels into four categories (low, med, high, and alert). Predictions of pollutant concentrations have been the subject of studies by other researchers.

Corani [5] an artificial neural network was developed to forecast O3 and PM10 concentrations using data from the previous day, and two different neural network models—a feed forward neural network and a pruned neural network—were compared. There have been new advancements made using Feed Forward Neural Networks.

Fu [6] suggests a Gray model in conjunction with a Rolling mechanism to enhance the performance of classic Feed Forward Neural Networks.

Jiang [7] air pollution prediction was a task put to many models (a chemical and physical model, a regression model, and a multi-layer perceptron), and the results showed that statistical models could do as well as their more conventional physical and chemical counterparts.

Ni, X. Y. [8] based their analysis of PM 2.5 data in the Beijing area on a comparison of several statistical models, and their findings suggested that linear regression models may be superior in certain circumstances than the other models. Converting regression tasks to classification tasks, however, is difficult since it leads to erroneous results because it disregards the scale of the numerical data.

III. PROPOSED METHOD

Data acquisition:

"If we want to evaluate the feasibility and accuracy of PM estimation based on image analysis, we need to build a database. We collected images taken in Beijing (China), Shanghai (China), and Phoenix (United States) for this research, along with their corresponding information, which included the time, PM2.5 index, temperature range, and latitude/longitude of each photograph (U.S.). The Beijing dataset consists of 327 photos, all shot on the same day of 2014 at the same time (early morning) and in the same general area (showing the Beijing Television Tower). Every hour from 8:00 a.m. to 16:00 p.m. from May through December of 2014, photographers all throughout Shanghai captured the city's iconic skyline, including the Oriental Pearl Tower, for the Archive of Many Outdoor Scenes (AMOS) collection."[9].

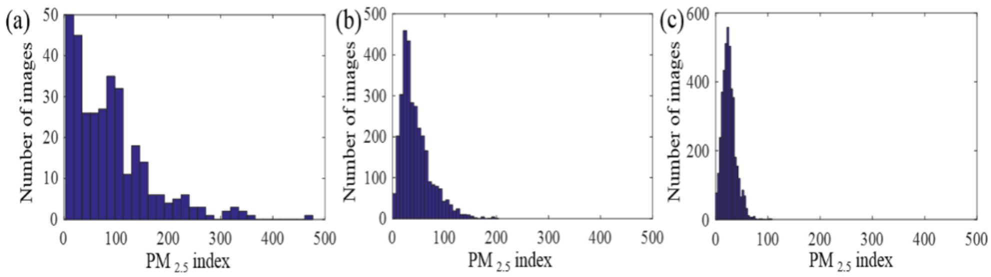

Fig 1. The histogram of $PM_{2.3}$ in different cities

The following image processing technique was used to estimate the PM2.5 index once the aforementioned database was constructed. The major phases of the process, shown in Fig. 3, are selecting areas of interest (ROIs), extracting features, training a regression model, and making predictions. Below, we outline the specifics of each of these measures.Fig 3.

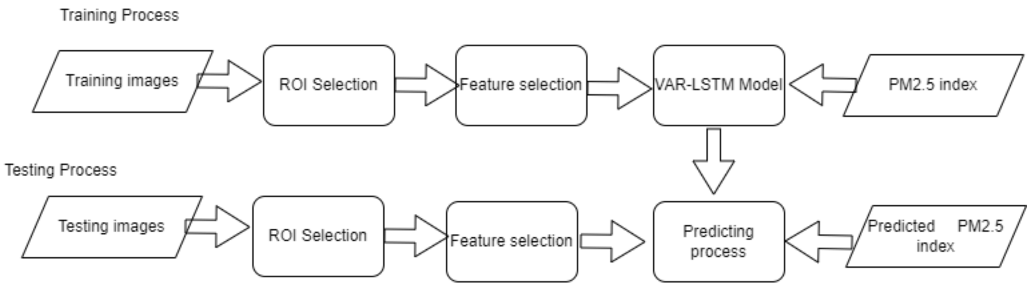

Fig 2. Architecture for image analysis and air pollution prediction from images

ROI Selection:

Initially, I will need to get rid of the watermarks on these images. Our photographs have watermarks that reveal the time and date they were captured; these watermarks are shown in white letters in the first and final rows. Next, a mask of the sky area is constructed, since this is visible in all three cityscapes. Fig. 4 displays three pictures that are emblematic of the three cities. It is easy to make out the buildings and the sky behind them. After the color photos were transformed to grayscale, the Otsu technique was used to transform them into binary. By choosing a threshold that either reduces intra-class variation or increases inter-class variance, the Otsu technique transforms grayscale pictures into binary ones. As the sky is more prominent than the buildings, it dominates the top half of the binary picture in these types of photographs. The blue lines in Fig. 4 demarcate the boundary between the sky and the buildings. We were able to get rid of the white-building-induced background hum by using the opening operator in conjunction with a 4x4 disk structuring element. To examine the transmission difference at various distances and PM concentrations, we manually design the ROIs for the distant buildings in the third step, as shown in Fig. 4.

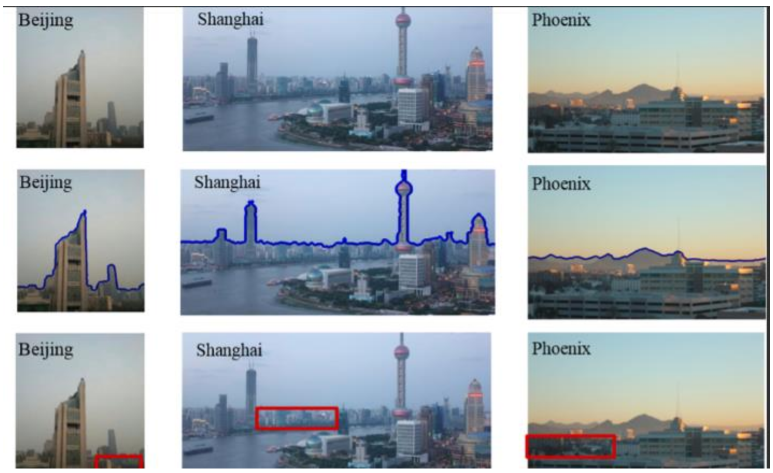

Fig 3. Sample photos in our haze detection dataset

Feature extraction:

According to the theoretical model described, scene brightness fading may be characterized by transmission. If we assume that all photos captured in the wild have some pixels with zero or extremely low intensity for at least one color channel, we may treat the transmission and, by extension, the attenuation, with a single fuzzy picture.

In the current model, it is assumed that as the distance from the camera increases, the transmission drops exponentially. By evaluating photos captured at varying distances, we were able to gauge the quality of the transmission. Figure 5A depicts four regions-of-interest (ROIs) denoted by red boxes, all of which correspond to buildings that are spaced increasingly further away from the camera. FIGURE 5: Four ROIs at varying distances, as shown by the transmission map. A semi-logarithmic plot of the average transmission values for the four ROIs demonstrates an exponential decline in transmission with increasing distance, providing more support for the accuracy of the Beer-Lambert law.

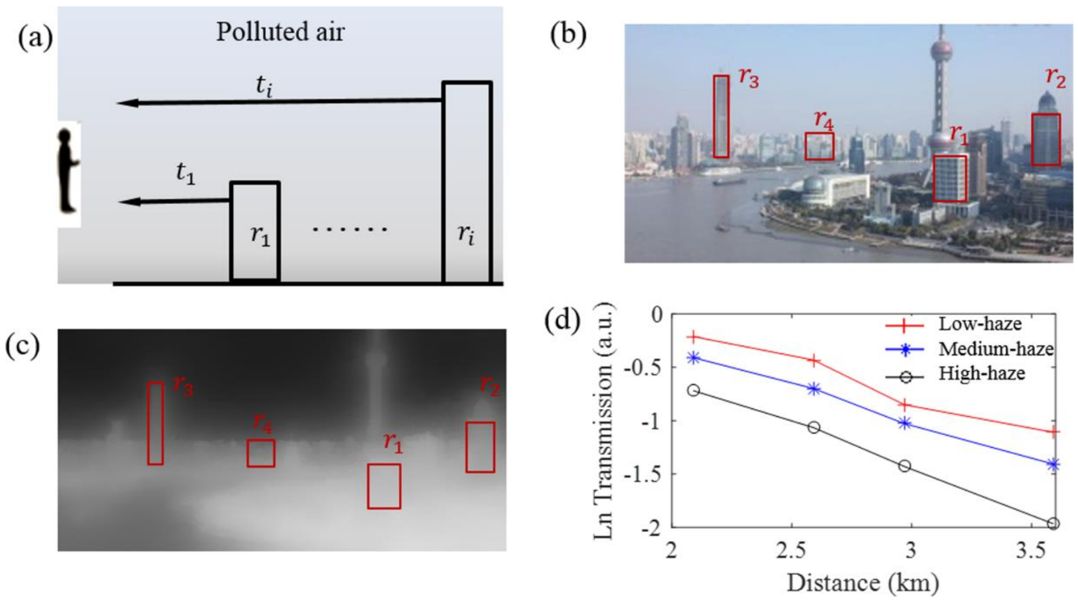

Fig 4. The transmission decreases as a distance or $PM_{2.5}$ index increases

Countless methods exist for evaluating an image's contrast. The root mean square (RMS) may be used to quickly explain the contrast in a picture. This method has been shown to agree with how people really see contrast in images. The root-mean-square contrast of a picture is calculated as the standard deviation of the pixel intensities.

$$RMS = \sqrt{\frac{1}{MN}\sum_{i=1}^{N}\sum_{j=1}^{M}(I_{ij} - avg(I))^2}$$

whereavg(I) is the average intensity across all pixels in the M by N image and Iij is the intensity at pixel position (i,j). Neither the RMS contrast value nor its distribution can be inferred from the spatial frequency content of the image.

Picture entropy, a measure of the amount of information in an image that is connected to its texture, is another aspect of images that may reveal PM information. The entropy of an image is defined as

$$entropy = -\sum_{i=1}^{M} p_i log_2 p_i$$

where p_i is the likelihood that pixel I has intensity I where M is the maximum value for pixel intensity in the picture. Image entropy falls as PM concentration rises, indicating that more and more information are being lost.

Vector Auto Regression model

Air quality factors are complex and dynamic relationships are present among the features [10]. The general simultaneous equations model has lower efficiency in revealing dynamic effects for exploringlag phase effects of explained variables of explanatory variables on its own. The available simultaneous equations have set variables as exogenous or endo generous variables that miss someimportant lag variables. Subjective settings in equations model error are reduced by considering allvariables as endogenous in the VAR model [11]. TheVAR model has the following advantages compared to the traditional single equation, (1) generality of the VAR model, and this is easy to add explanatory variablesdue to this is not based on theories. (2) VAR model reveals the short-term and long-termrelationship between air quality factors. The VAR models have limitations, such as many parameters are required to measure, and high correlation in explanatory variables lag periods. There are many complex interrelationships between the factors that cause CO2 emissions and the emissions themselves, as shown by the research.The VAR model is used for dynamic effects analysis of the drivingforce of CO2 emissions.

Below Equation provides the formula for the VAR model

$$y_t = \vartheta + A_1 y_{t-1} + \cdots \ldots \ldots \ldots .. + A_p y_{t-p} + \mu_t, t = 0, 1, 2$$

where random vector ($K \times 1$) is in $yt = (y1t , \ldots , ykt)'$, coefficient matrix of ($K \times K$) is denoted as Ai , intercept terms of ($K \times 1$) vector is denoted as $v = (v1, \ldots , vk)'$.

Long Short Term Memory

The LSTM can retain the important information for the long term based on cell and forget gate. Classifying arrhythmia signals calls for both real-time and historical information. Because of its ability to deal with difficulties of long-term dependencies using a self-feedback mechanism that operates on a hidden layer, the LSTM model has shown to be useful [12, 13].Memory cell and three gates, such as input, forget, and output gates, were used to store information in the LSTM model to help handle the problem of long-term features [14, 15].

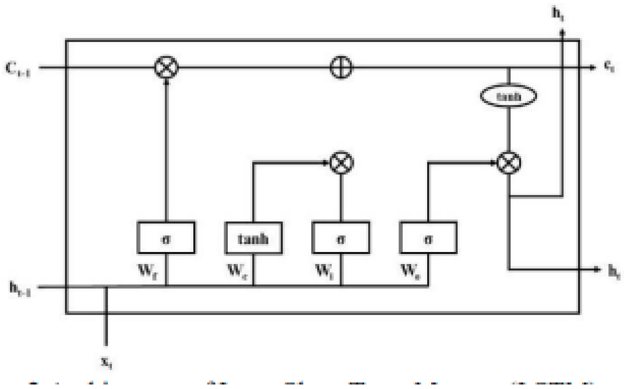

Fig 5. Architecture of Long Short Term Memory Model

Combination of LSTM and VAR

Neural network training is improved based on the fitted VAR model. Multivariate data of internal behavior of VAR model for adjusting insane values of multivariate data correcting reconstructing NaNs correctly and anomalous trends. Fitness value contains information that is modified original data version manipulated in the model during the training procedure. The kind of augmented data of source original train.

A two-step training process is in this strategy. One-step forecasting of all series is carried out using the feeding LSTM model and VAR fitted values. Training with raw data is the same differential data to fit VAR. LSTM handles external data sources, for instance, weather conditions or attributes like months, hours, and weekdays to encode cyclically.

A neural network learns from two different data sources and provides better performance on test data.The Vanishing Gradient Problem needs to be handled through multiple steps training. If two tasks are applied to a neural network, the network forgets the first task, and this is a common problem in neural networks.

Results and Discussion:

We analyzed the relapse model's capability to predict the PM2.5 list by randomly assigning certain cases to the training set and others to the testing set. We utilized two-fold cross-approval to predict the data for each city. In Fig. 6, we see a comparison between the PM2.5 list that was intentionally compiled and the PM2.5 list that was generated automatically. The accuracy of the predictions was analyzed using the Root mean square error (RMSE), R-squared, and the F-test.To explain what RMSE is, we say,

$$RMSE = \sqrt{\frac{1}{N}\sum_{i=1}^{N}(y_i - \widehat{y_i})^2}$$

"Where $\hat{y}_i$ is the ith forecast value, and y_i is the ith observed value, i = 1,2,…,N. R-squared is given by

$$R^2 = 1 - \frac{\sum_{i=1}^{N}(y_i - \widehat{y_i})^2}{\sum_{i=1}^{N}(y_i - avg(y))^2}$$

where $\hat{y}_i$ is the ith forecast value, $avg(y)$ is the average value, y_i is the ith observed value, $i = 1,2,\ldots,N$."R-squared increases as our knowledge of the discrepancy between the model's forecast and the observed result grows; a value of 1 indicates a perfect fit between the gauge and the observed result.The F-test contrasts the likelihood of a situation where all relapse coefficients equal 0 with the likelihood of a situation where at least one does not.The observed reliability of the R-squared measures is supported by the significance of the F-test. Fig 6. The answers are (a) Beijing, (b) Shanghai, and (c) Phoenix.

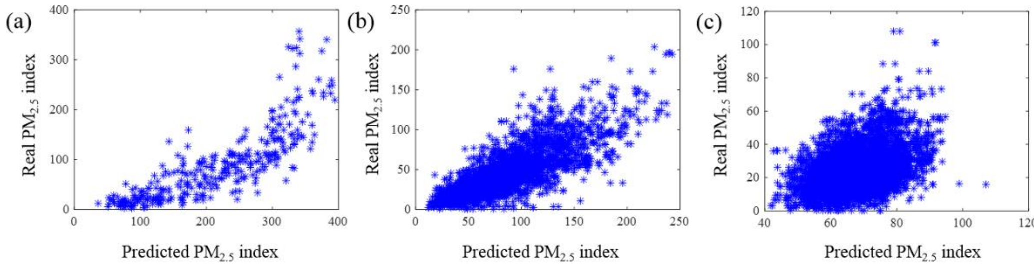

Fig 6. Real $PM_{2.5}$ index vs. predicted $PM_{2.5}$ index plot

To illustrate this, Fig. 6 displays a strong correlation between the predicted and measured PM2.5 indices for Beijing and Shanghai. For Phoenix, on the other hand, the association is less clear since the PM2.5 level there is quite stable (0–40). Phoenix has the worst air quality of any major city in the United States, with a PM2.5 index of 38. In comparison, the PM2.5 index in Beijing and Shanghai may reach up to 340 and 204, respectively. Given that Figure 6A illustrates the prediction error for high PM2.5 index data, the finding that Beijing has a higher RMSE than Shanghai is not surprising. This means that the R-squared values in Beijing and Shanghai are higher than those in Phoenix for the same reasons given before. The F-test shows that the Table 1 R-squared values are credible.

"Dataset	**RMSE**	**R squared**	**F test**
Beijing	43.62	0.64	P<0.0001
Shanghai	20.23	0.57	P<0.0001
Phoenix	2.34	0.23	P<0.0001

Table 1. Assessment of the VAR – LSTM"

CONCLUSION:

The PM2.5 index in the air was estimated using an image-based approach. Detailed PM2.5 data for Beijing, Shanghai, and Phoenix were recovered, and a wide range of image attributes were analyzed, including transmission, picture difference and entropy, sky perfection and variation. "Researchers in Beijing (using 327 images, one for each day of the study's 327-day duration), Shanghai (1954 images, or 8 images per day for 245 days), and Phoenix (using 4306 images, or 16 images per day for 270 days) used picture and non-picture elements to analyze countless images and found that the method could provide a reasonable expectation of PM2.5 file across a broad PM2.5 list range. The current technology will not replace the gold standard molecule counting instrument, but its portability and compatibility with mobile devices could help bring issues of air contamination to light and warn patients with severe respiratory conditions to avoid areas where being present is illogical.

REFERENCES:

1. Wang H, Yuan X, Wang X, Zhang Y, Dai Q. Real-time air quality estimation based on color image processing. IEEE Conference on Visual Communications and Image Processing; 2014 Dec 7–10; Valletta, Malta; 2014. p. 326–329.
2. Hyslop NP. Impaired visibility: the air pollution people see. Atmos Environ. 2009; 43(1): 182–195.
3. Athanasiadis, I.N.; Kaburlasos, V.G.; Mitkas, P.A.; Petridis, V. Applying machine learning techniques on air quality data for real-time decision support. In Proceedings of the First international NAISO Symposium on Information Technologies in Environmental Engineering (ITEE'2003), Gdansk, Poland, 24–27 June 2003.
4. anidas, E.; Avouris, N. Short-term air quality prediction using a casebased classifier. Environ. Model. Softw. 2001, 16,pp. 263–272.
5. Corani, G. Air quality prediction in Milan: Feed-forward neural networks, pruned neural networks and lazy_learning. Ecol. Model, 185,pp. 513–529.2005.
6. Fu, M.; Wang, W.; Le, Z.; Khorram, M.S. Prediction of particular matter concentrations by developed feed-forward neural network with rolling mechanism and gray model. Neural Comput. Appl., 26, pp.1789–1797, 2015.
7. Jiang, D.; Zhang, Y.; Hu, X.; Zeng, Y.; Tan, J.; Shao, D. Progress in developing an ANN model for air pollution_index forecast. Atmos. Environ. 2004, 38, 7055–7064.
8. Ni, X.Y.; Huang, H.; Du, W.P. Relevance analysis and short-term prediction of PM 2.5 concentrations in Beijing based on multi-source data. Atmos. Environ., 150, pp.146–161, 2017.
9. Jacobs N, Roman N, Pless R. Consistent temporal variations in many outdoor scenes. CVPR 2007: Proceedings of IEEE Conference on Computer Vision and Pattern Recognition; 2007 Jun 17–22; Minneapolis, USA; 2007.
10. A. Hernandez-Matamoros, H. Fujita, T. Hayashi,and H. Perez-Meana, "Forecasting of COVID19 per regions using ARIMA models and polynomial functions", Applied soft computing, Vol. 96, pp. 106610, 2020.
11. S.N. Singh, and A. Mohapatra, "Repeated wavelet transform based ARIMA model for very short-term wind speed forecasting", Renewable energy, Vol. 136, pp. 758-768, 2019.
12. A. Sherstinsky, "Fundamentals of recurrentneural network (RNN) and long short-term memory (LSTM) network", Physica D: Nonlinear Phenomena, Vol. 404, pp. 132306, 2020.
13. V.K.R. Chimmula, and L. Zhang, "Time series forecasting of COVID-19 transmission in Canadausing LSTM networks", Chaos, Solitons& Fractals, Vol. 135, pp. 109864, 2020.

14. F. Shahid, A. Zameer, and M. Muneeb, "Predictions for COVID-19 with deep learning models of LSTM, GRU and BiLSTM", Chaos, Solitons& Fractals, Vol. 140, pp. 110212, 2020.